X-rays minibeam radiation therapy at a conventional irradiator: Pilot evaluation in F98-glioma bearing rats and dose calculations in a human phantom

Marios Sotiropoulos, Elise Brisebard, Marine Le Dudal, Gregory Jouvion, Marjorie Juchaux, Delphine Crépin, Catherine Sebrie, Laurene Jourdain, Dalila Labiod, Charlotte Lamirault, et al.

Clinical and Translational Radiation Oncology 27 (2021) 44–49

Contents lists available at ScienceDirect

Clinical and Translational Radiation Oncology

journal homepage: www.elsevier.com/locate/ctro

X-rays minibeam radiation therapy at a conventional irradiator: Pilot evaluation in F98-glioma bearing rats and dose calculations in a human phantom

Marios Sotiropoulos [a,1], Elise Brisebard [b,c,1], Marine Le Dudal [b,d], Gregory Jouvion [b], Marjorie Juchaux [a], Delphine Crépin [e], Catherine Sebrie [f], Laurene Jourdain [f], Dalila Labiod [g], Charlotte Lamirault [g], Frederic Pouzoulet [g], Yolanda Prezado [a,*]

[a] Institut Curie, Université PSL, CNRS UMR3347, Inserm U1021, Signalisation radiobiologie et cancer, 91400 Orsay, France
[b] Institut Pasteur, Neuropathologie Expérimentale, 75015 Paris, France
[c] Laboratoire d'Histopathologie, VetAgro-Sup, Université de Lyon, Marcy l'Etoile, Lyon, France
[d] Ecole Nationale Vétérinaire d'Alfort, Biopôle, Unité d'Histologie, d'Embryologie et d'Anatomie Pathologique Université Paris-Est, Maisons-Alfort, France
[e] Laboratoire de Physique des 2 Infinis Irène Joliot-Curie (IJCLab-UMR 9012), CNRS/Université Paris-Saclay/Université de Paris, Campus Universitaire, Orsay, France
[f] BIOMAPS Université Paris-Saclay, CEA, CNRS, Inserm, Service Hospitalier Frédéric Joliot, 91401 ORSAY, France
[g] Translational Research Department, Experimental Radiotherapy Platform, Institut Curie, PSL Research University, University Paris Saclay, Orsay, France

ARTICLE INFO

Article history:
Received 7 October 2020
Revised 4 January 2021
Accepted 4 January 2021
Available online 8 January 2021

Keywords:
Minibeam radiation therapy
Tabletop systems
High-grade gliomas

ABSTRACT

Minibeam radiation therapy (MBRT) is a type of spatial fractionated radiotherapy that uses submillimetric beams. This work reports on a pilot study on normal tissue response and the increase of the lifespan of glioma-bearing rats when irradiated with a tabletop x-ray system. Our results show a significant widening of the therapeutic window for brain tumours treated with MBRT: an important proportion of long-term survivals (60%) coupled with a significant reduction of toxicity when compared with conventional (broad beam) irradiations. In addition, the clinical translation of the minibeam treatment at a conventional irradiator is evaluated through a possible human head treatment plan.

1. Introduction

Minibeam radiation therapy (MBRT) is an innovative technique based on a spatial modulation of the dose [1,2]: the irradiation is carried out with one or several arrays of submillimetric (500–700 μm) wide beams, resulting in dose profiles consisting of a succession of areas of high dose (peaks) followed by areas of low doses (valleys). MBRT was originated at large synchrotrons [1], where it has shown a remarkable preservation of normal rat brain [1,3–6] while an increase of mean survival time in glioma-bearing rats was observed [4,7].

Despite its promises, the exploration of MBRT was limited due to limited access to synchrotrons until its recent implementation at small animal irradiators [5,6]. This offers the possibility of a widespread use of the technique, which would allow performing systematic comprehensive radiobiological evaluations.

In contrast to some other implementations, our setup enables the irradiation of intracranial tumours [5]. This work aimed at assessing the gain in therapeutic index in glioma-bearing rats provided by our table-top system. For that purpose, both the response of normal rats to two dose levels and the increase of lifespan of F98-glioma bearing rats were evaluated. Furthermore, the clinical translation of the minibeam treatment at a conventional x-ray irradiator was assessed assessed. For this evaluation, a first dose calculation in a human-head phantom in the same tabletop system was performed.

2. Materials and methods

All animal experiments were conducted in accordance with the animal welfare and ethical guidelines of our institutions. They were approved by the Ethics Committee of the Institut Curie and French Ministry of Research (permit no. 6361–201608101234488). Rats were anaesthetised with isoflurane (2.5% in air) during irradiation and magnetic resonance imaging (MRI). At the end of the study, the rats were terminally anaes-

* Corresponding author.
E-mail address: yolanda.prezado@curie.fr (Y. Prezado).
[1] Equally contributed.

https://doi.org/10.1016/j.ctro.2021.01.001
2405-6308/

thetised for brain fixation by the intracardiac perfusion of formalin zinc.

2.1. Tumor cell line and tumor implantation

A rat glioma cell line, F98 (ATCC-2397TM) transfected with the luciferase gene, was used. A number of 10,000 F98-Luc cells were suspended in 5 μl DMEM and then injected intracranially into male Fischer 344 rats (Janvier Labs) using a Hamilton syringe through a burr hole in the right caudate nucleus (5 mm anterior to the ear-bars, i.e. at the bregma site, 3.0 mm lateral to the midline, and 5.5 mm depth from the skull).

Tumor presence was verified by means of Bioluminescence Imaging (BLI) at an IVIS spectrum (PerkinElmer). For the BLI procedure the rats were injected intraperitoneally with a concentration of 150 mg/kg (P/N 122799) of D-luceferin (PerkinElmer) in 500 μl. The irradiations took place 11 days after tumor implantation.

2.2. Irradiations and dosimetry

The irradiations were performed using our implementation at a small animal irradiator [5]. All groups received unilateral irradiations with an array of 12 mm-high planar minibeams with a 700 ± 20 μm-width and 1465 ± 10 μm centre-to-centre spacing at 1 cm depth in a water phantom. The measured dose rate at the central peak of the array at 1 cm depth in a water phantom was 3.37 ± 0.13 Gy/min. Five groups of rats (7 weeks-old at the moment of irradiation) were considered. Table 1 shows the characteristics of the groups and the doses received. The doses received by the group of tumor-bearing rats (group 5) and the group of normal rats receiving the lowest doses (group 2) were equal, within the uncertainty bars. Doses were assessed using Gafchromic films and Monte Carlo simulations in a rat's computed tomography image [8]. No broad beam irradiations were performed as it has been shown that even 20 Gy with a broad beam would have been largely toxic [5,9], while a mean dose of 20–25 Gy is needed to obtain long-term survivals [10].

A dose response study in normal rats was carried out in a first experiment. The tolerable dose, out of the two evaluated, was then used in the second experiment to treat tumor-bearing rats to assess if that dose was high enough to obtain a significant tumor control effectiveness. One-single fraction scheme was used to avoid any possible blurring inter-fraction of the minibeam pattern due to positioning errors.

Gafchromic films were placed laterally on each side of the rat's head (beam entry and exit) and attached to the skin. The films allowed the assessment of the irradiation quality, confirming the minibeam pattern.

2.3. Animal follow up

The follow up lasted for 6 and 4 months in the case of normal and tumor-bearing rats, respectively. The clinical status of the animals was checked 2 and 5 times per week in the case of normal and tumour-bearing rats, respectively. Concerning normal rats, the endpoints of the study were: rapid body weight loss reaching 20% at any time or 15% in 3 days, hyper-reactivity, prostration, signs of lack of grooming (hair unkempt, dirty), locomotion disorders and breathing difficulties. Concerning tumour-bearing rats, any rat showing the classical adverse neurological signs related to the tumour growth in the brain was humanely killed. These signs could be any of the following: loss of appetite and substantial weight loss (>10% of the weight in 24 h), periorbital haemorrhages, seizures or prostration.

Normal rats underwent an anatomical MRI study at 10 days after irradiation (n = 3/group), and at the end of the study (n = 5/-group). For each imaging session, a catheter was inserted into the tail vein for contrast agent administration. The image acquisitions were performed at a 7-Tesla preclinical magnet (Bruker Avance Horizontal 7-T Bruker, Inc., Billerica, MA) equipped with a 35-mm-diameter "bird-cage" antenna. The sequences described in Prezado et al. [5] were used.

During necropsy, the brain fixed by intra-cardiac perfusion of a fixative solution (formalin zinc) was removed and placed in the fixative before being embedded in paraffin. Several sections of the right and left sides of the brain were cut: one parasagittal section level for groups 1, 4, 5 (for the rats with easily detectable tumors in the group 5), and six parasagittal section levels separated by 200 μm, followed by coronal sections, for groups 2, 3 and 5 (for the rats with no detectable tumors in the group 5). The sections were stained in hematoxylin and eosin (HE) to detect and describe the lesions or the tumors. Immunohistochemistry (IHC) analysis was performed to assess the networks and cell morphologies of microglial cells (anti-Iba-1 antibody, Wako Chemicals, dilution: 1:500) and astrocytes (anti-GFAP antibody, Sigma-Aldrich, dilution: 1:500). Microglial cell morphology is indeed linked to their physiological state; neuroinflammation is characterized by "reactive" microglial cells displaying a larger cell body and thicker cell processes. They can also be grouped as clusters (microglial nodules) in the tissue. Immunohistochemistry analyses were performed with a BOND RX Autostainer (Leica Biosystems), using the BOND Intense R Detection Kit (Leica Biosystems, ref: DS9263). The analyses were carried out by 3 trained veterinary pathologists (blind analysis).

2.4. Calculations in a human phantom

A first evaluation on a human brain tumour treatment with the same tabletop system was also performed by means of Monte Carlo simulations. The TOPAS Monte Carlo simulation toolkit [15], version 3.2, was used. The x-ray minibeam source and collimation geometry were the same as previous works [5,8]. Two different energies were considered: 220 and 300 kV. The first one is the current energy of the system, the second one is available in some other models.

The head of the International Commission on Radiological Protection (ICRP) male phantom [16] was imported in TOPAS, with the material composition as given in the ICRP report. See Fig. 1. A virtual tumour in the centre of the brain was considered. The tumour was targeted with four beams: two opposite lateral minibeam arrays and two other in the orthogonal (coronal) direction. The centre-to-centre distance (ctc) was a factor of two larger than in the animals' experiments. The dose to water was scored with a voxel size of 1.85 mm × 0.1 mm × 1.84 mm. A number of 3.6 $x10^{11}$ primary photons sampled from the energy spectrum were simulated for each minibeam field. To improve the computational efficiency, photons from the spectrum below 21 and 30 keV for the 220 and 300 kV spectrum respectively were not simulated. The spectrum was discretized with bin size of 1 keV. The "g4em-standard_opt3" physics list was selected, and a cut-off of 0.005 mm was used in the scoring volume.

3. Results

3.1. Normal rats

All normal rats gained weight along the study. However, the gain rate was slightly lower in group 3 (highest dose): a factor 1.3 ± 0.1 mean gain between the day of irradiation and the end of the study was observed. In contrast, groups 1 (controls) and 2 (lowest dose) gained weight at the same rate within uncertainty

Table 1
Groups and doses received.

Group	Number of rats	Dose at 1 cm-depth in the rat		
		Peak dose	Valley dose	Mean
1. Normal rats-controls	5	0 Gy	0 Gy	0 Gy
2. Normal rats-irradiated (lowest dose)	6	57 ± 5 Gy	5.0 ± 0.3 Gy	20 ± 2 Gy
3. Normal rats-irradiated (highest dose)	5	81 ± 6 Gy	7.2 ± 0.6 Gy	28 ± 2 Gy
4. Tumor-bearing rats-controls	5	0 Gy	0 Gy	0 Gy
5. Tumor-bearing rats-irradiated	5	65 ± 6 Gy	5.8 ± 0.5 Gy	22 ± 2 Gy

Fig. 1. The minibeam collimator field projected on the middle sagittal slice of the DICOM version of the ICRP phantom. The colours are inverted, i.e. denser materials represented by darker colour.

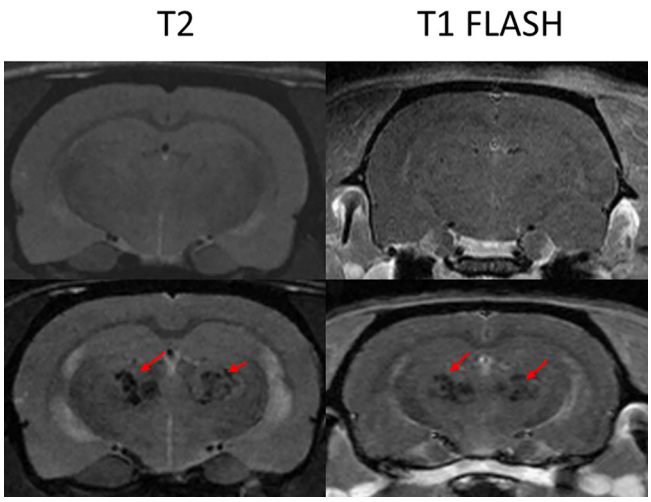

Fig. 2. The upper row shows the T2 and T1 FLASH 5 min after Gd injection images of one of the animals in group 2 (upper row) and another one in group 3 (lower row). While no lesions are observed in the MRI images of group 2, large lesions, which could be compatible with necrosis, are observed in group 3.

bars: a ratio of 1.7 ± 0.2 (controls) and 2.0 ± 0.3 (MBRT) between the day of irradiation and the end of study. The ANOVA-test performed showed a significant difference between group 3 and the other two ($p = 0.0004$). No irradiated animal exhibited any skin damage.

No evident pathology/lesions was observed in the MRI acquisitions at 10 days post irradiation. Six months after irradiation, MRI revealed severe lesions in both brain hemispheres in group 3. No lesions were detected in group 2. See Fig. 2.

Histopathological analyses revealed different lesion profiles between the groups (Fig. 3). Concerning group 2 (lowest dose), most rats (4/6) displayed only minimal to mild lesions: oedema, small foci of mineralisation (<100 μm), apoptotic neurons (to distinguish from dark neurons, i.e. artefacts due to fixation procedures), and small foci of reactive microglial cells. Only 2 rats displayed larger and/or multifocal destruction/mineralisation in the thalamus. Concerning group 3 (highest dose), lesions were marked to severe, with large (>500 μm) foci of neuropil destruction/mineralisation observed in all the rats (5/5), mostly in the thalamus and the cortex. No lesion was observed in rats from group 1.

3.2. Tumour-bearing rats

Fig. 4 shows the survival curves for groups 4 and 5 (tumour-bearing rats). The median survival time of the control group was 26 ± 5 days. A significant increase in survival of irradiated rats with respect to controls was observed ($p = 0.009$). Sixty per cent (3/5) of the animals lived for the whole duration of the study (4 months).

All animals in the control group exhibited tumours, more often invading the thalamus and vertices, and less often the meninges and brain stem, with necrosis, cavitation and a severe and extensive microglial cell reaction (Fig. 5).

No tumour tissue was observed on the examined histopathological sections, but the rats displayed ventriculomegaly (3/3), foci of necrosis/cavitation with mineralisation (most often in the thalamus, 3/3), marked microglial cell reaction and activation of astrocytes, especially in/around the necrotic/mineralised foci (3/3). Only the two irradiated rats, which reached an endpoint and needed to be sacrificed at early times, displayed large tumours. Whole-slide scan images of histological sections for all the animals of this part are available in Supplementary data.

3.3. Calculations in a human-head phantom

The promising results obtained encouraged us to perform a first calculation of the dose distributions in a human-head phantom. Fig. 6 shows a 2D coronal and sagittal view of the dose distributions. The spatial fractionation is maintained in depth. The peak-to-valley dose ratio (PVDR) at the coronal plane, approximately at 3.7 cm depth, between the skin and the beam crossing area, is 4.9 ± 0.1 for 220 kV and 4.7 ± 0.1 for 320 kV. The PVDR is lower than the one in the normal rat brains of the experiments presented in this work, but it is equivalent to previous animals' experiments, which has shown a good normal tissue tolerance [9]. Additionally, the PVDR in normal tissues could be further increased by optimising the beam spacing. The PVDR at the centre of the brain, in the beam crossing area, is 5.2 ± 0.1 and 4.9 ± 0.1 for 220 and 320 kV, respectively, thus lower than the experiment reported in this work, so a higher tumour control could be expected from that point of view. The dose in the tumour could be increased by using contrast agents [10]. The two energies lead to very similar values of PVDR.

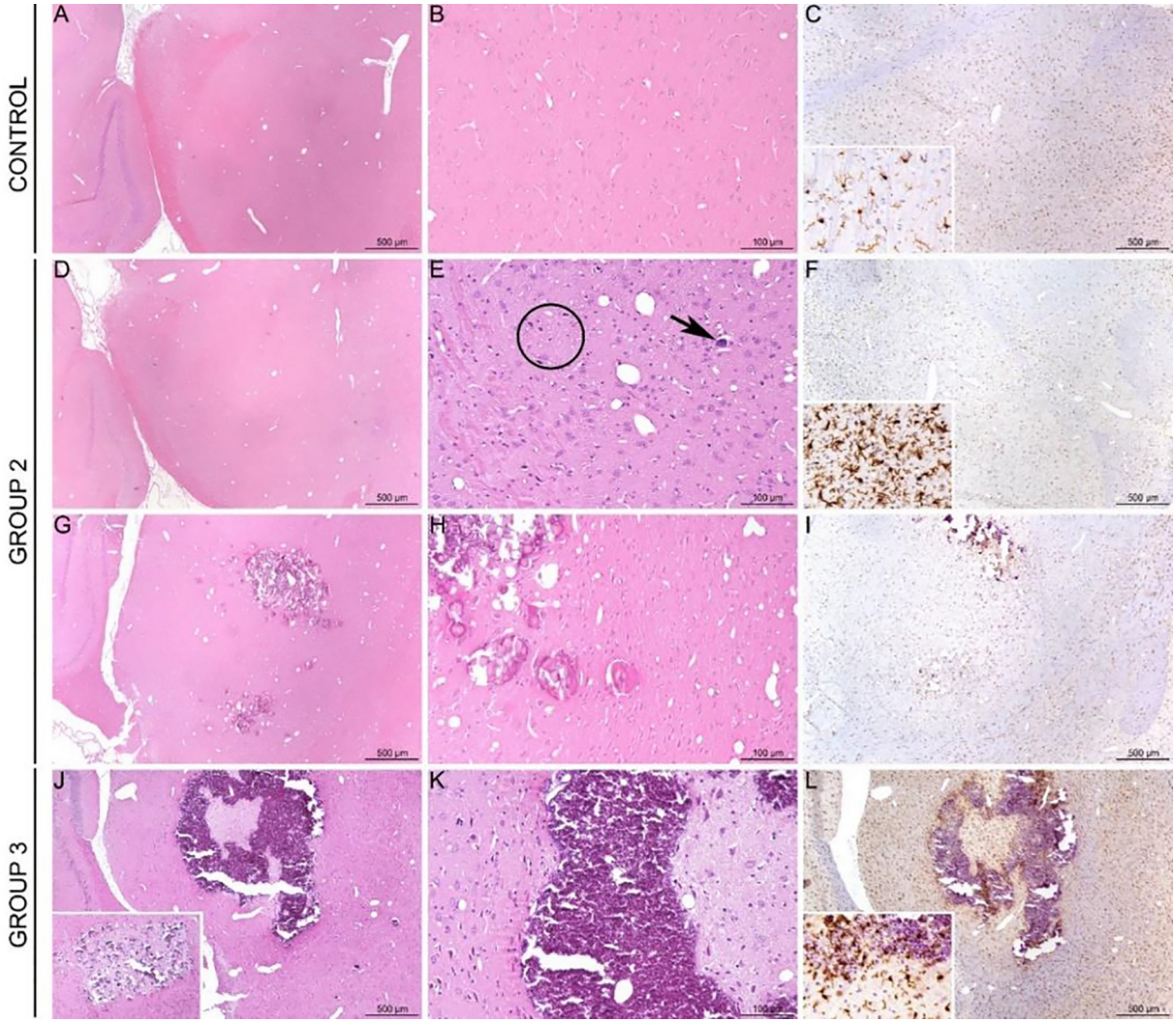

Fig. 3. Histopathological impact of irradiation (low and high doses) in normal rats. Control rats (A-C) did not display any histological lesion. Most rats from the group 2 (lowest dose; D–F) displayed only minimal to mild lesions with apoptotic neurons (black circle), small foci of mineralisation (black arrow) (E), and only small foci of microglial cell reactivity (F, inset). Two rats displayed more severe lesions (G-I), characterized by multifocal destruction/mineralisation of the thalamus (G-H) with peripheral reaction of microglial cells (I). In contrast, all rats from group 3 displayed large destruction/mineralisation located mostly in the thalamus (J-K) and cortex (J; insert), also with peripheral microglial cell reaction (L). A, B, D, E, G, H, J, K: HE staining. C, F, I, L: anti-Iba-1 IHC.

However, the highest one results in around 30% lower dose deposition in the bone for the same dose deposited in the target.

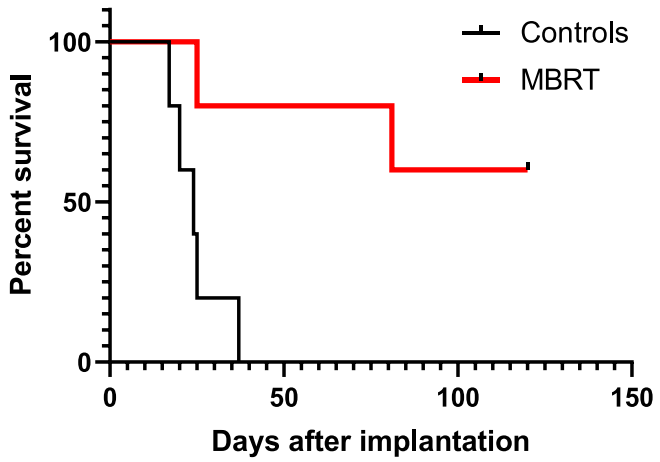

Fig. 4. Survival curves for the controls and irradiated animals.

4. Discussion and conclusions

Normal tissue tolerances remain the main limiting factor for a satisfactory treatment of radioresistant tumours, such as high-grade gliomas. Spatially fractionated radiotherapy has shown promise to diminish the normal tissue complication probabilities. MBRT had demonstrated a gain in normal tissue tolerances both at synchrotron [3] and at our tabletop system [5]. The aim of this study was to investigate the feasibility of x-ray minibeams in a conventional irradiator. A dose response study was performed to determine the level of doses, that, while being still tolerable, lead to a significant increase in lifespan compared to non-irradiated controls. Furthermore, the feasibility of the conventional irradiator for human minibeam radiation therapy was evaluated by using a human head dosimetry study.

Despite being a pilot study, this work provides, for the first time, evidence of the gain in therapeutic index of MBRT in glioma-bearing rats in a tabletop system. An important proportion (60%) of the animals survived for the whole duration of the study (4 months) and that, with a highly heterogeneous target dose coverage. No tumour tissue was observed on the examined

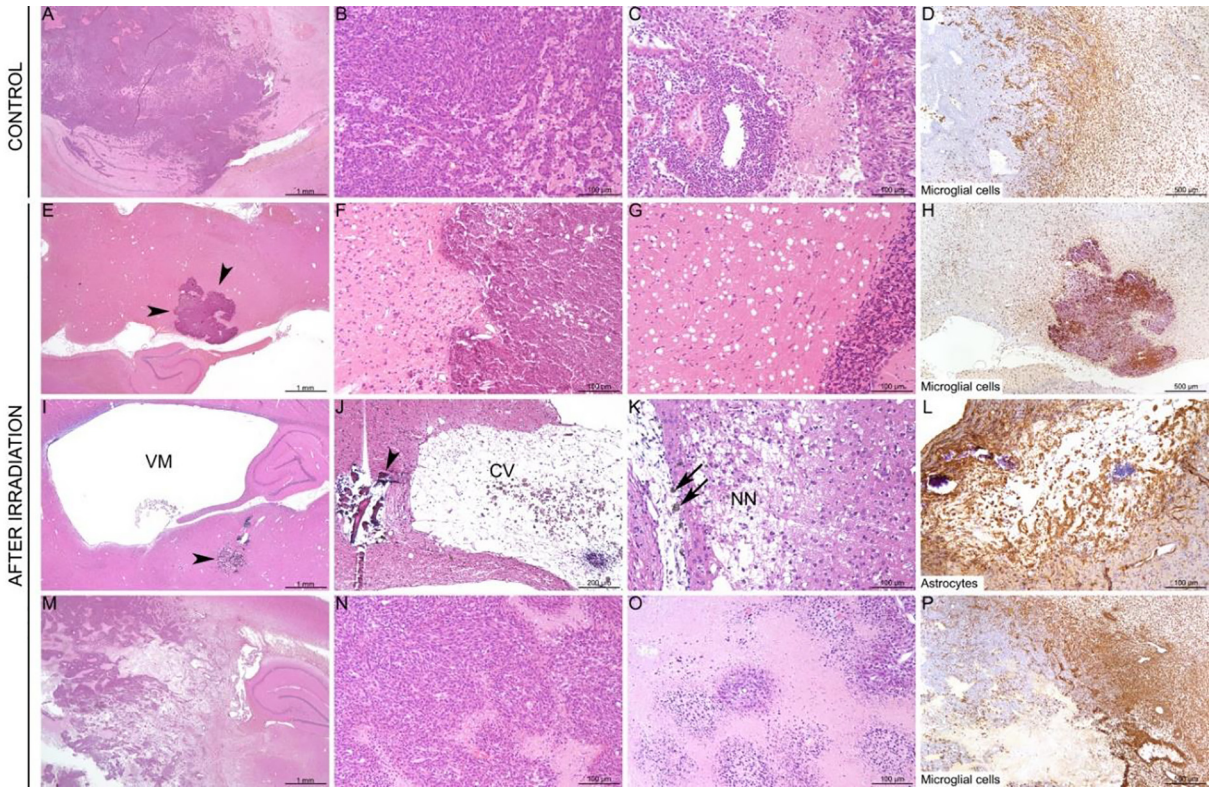

Fig. 5. Histopathological impact of irradiation in tumour-bearing rats. Control rats (A–D) displayed voluminous invading tumours, with large foci of necrosis and strong microglial cell reactivity (D). After irradiation, 3/5 rats survived, and no tumours were detected in the brain sections performed (E–L). These rats displayed: foci of mineralisation (E–F, arrowheads), extracellular oedema (G), strong microglial cell reactivity (H), ventriculomegaly (I, VM), necrosis with cavitation (J, CV) and mineralisation (I, J, arrowheads), focal destruction and necrosis of the neuropil (K, NN) with infiltration of macrophages containing brown pigment (K, black arrows), and activation of astrocytes, especially in the necrotic foci (L). Only 2/5 irradiated rats displayed voluminous tumours (M–N), with large central areas of necrosis (O) and marked peripheral activation of microglial cells (P). A–C, E–G, I–K, M–O: HE staining. D, H, P: anti-Iba-1 IHC. L: anti-GFAP IHC.

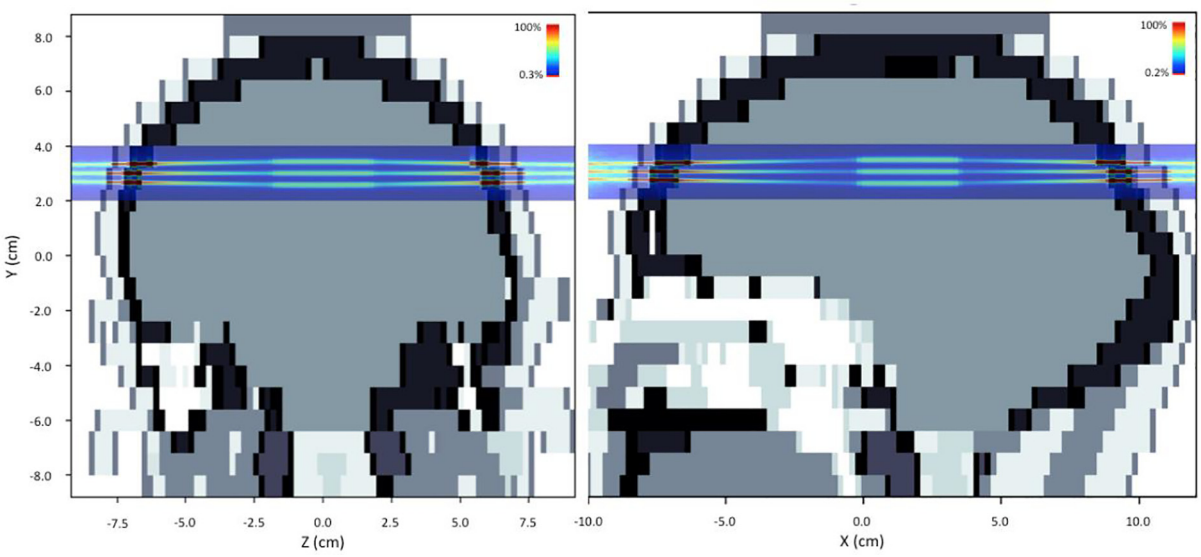

Fig. 6. 2D dose distributions in the coronal (left) and sagittal (right) planes.

histopathological sections. In contrast, lower long-term survival was obtained in previous evaluations of the response of F98-glioma bearing rats at the European Synchrotron Radiation Facility (ESRF) [4]. In those studies, the tumour bearing animals were irradiated with interlaced MBRT (quasi-homogenous dose distributions in the target) with a similar peak dose (54 Gy) as in our study [4]. Furthermore, the survival rate obtained in our study is higher than the long-term survival obtained with F98-bearing rats irradiated with a mean dose of 25 Gy by a broad beam [10].

The evaluation of the normal tissue tolerance was performed at the same dose as the tumour-bearing rat (*group 2, mean dose 20 ± 2 Gy*) and revealed reduced toxicity with respect to broad

beam irradiations [5]. In contrast, in our previous work [5], we observed extensive brain damage, including large radionecrosis in normal rats receiving 20 Gy mean dose in broad beam configuration. Since radiation doses higher than 20 Gy are reported to be needed to obtain long-term survivals in glioma-bearing rat experiments [10–12] in broad beam irradiation, we can postulate that MBRT could offer an increase of therapeutic index with respect to conventional irradiations.

In addition, an upper dose threshold (<80 Gy and 7 Gy peak and valley dose, respectively, at 1 cm depth in the rat head) could be established. At that level of dose, extensive brain damage is observed. Previous evaluations performed at synchrotrons seemed to indicate a higher dose tolerance in similar configurations [3]. Doses as high as 100 Gy peak dose (7 Gy valley dose) seemed to be well tolerated by normal brain. The difference in the results obtained with our tabletop system with respect to those at the ESRF synchrotron might be attributed to the FLASH effect (the dose-rate at the ESRF could reach 10,000 Gy/s [3,13]).

In the dose calculations at the human head phantom the PVDRs are lower than the PVDR in our preclinical study, although within the range reported in previous studies [5]. For example, Prezado et al [5] noted that the divergence of the beam leads to sharp decrease of the PVDR values for collimators very similar to the one used in this study. They reported a PVDR of 2.7 ± 0.1 at 5 cm depth in water. In our simulations, by using 4 cross-fired fields, we kept the PVDR in the centre of the tumour at about 5; where the centre of the tumour is at about 8–10 cm, depending on the direction. That brings the PVDR at a comparable value with the preclinical experiments, demonstrating the translational capabilities of the setup. A high mechanical precision (<1 mm) would be requested to deliver this cross-fired irradiation geometry. However, the requirements in terms of mechanical precision are reduced as to compare with interlaced irradiations and it could be achieved with high-precision goniometers.

These results also provide the basis for continuing the study of this technique. Future perspectives include comprehensive radiobiological evaluations to unravel the biological mechanisms involved in MBRT as well as work on technological evolutions to incorporate MBRT to patient's treatments. The later could involve designing a system based on the use of a higher energy and higher power tube than the one used in this study; such as the one recently proposed for the combination of FLASH and MBRT at the SARRP system [14].

Declaration on Competing Interest

One of the authors (YP) holds a patent on the implementation of MBRT in a small animal irradiator.

Acknowledgements

This research was performed with financial support from ITMO Cancer AVIESAN (Alliance Nationale pour les Sciences de la Vie et de la Santé, National Alliance for Life Sciences and Health) within the framework of the Cancer Plan (2009–2013), under grant agreement PC201327 and SIRIC 2018-2022: INCa-DGOS-Inserm_12554. We acknowledge PRACE for awarding us access to the computational cluster Joliot Curie-SKL (France) under the grant agreement 2019204903.

Appendix A. Supplementary data

Supplementary data to this article can be found online at https://doi.org/10.1016/j.ctro.2021.01.001.

References

[1] Dilmanian FA, Zhong Z, Bacarian T, et al. Interlaced X-ray microplanar beams: a radiosurgery approach with clinical potential. Proc Natl Acad Sci USA 2006;103:9709–14.
[2] Prezado Y, Renier M, Bravin A. A new method to generate minibeam patterns. J Synchrotron Radiat 2009;16:582–6.
[3] Prezado Y, Deman P, Varlet P, Jouvion G, Gil S, Le Clec'H C, et al. Tolerance to dose escalation in minibeam radiation therapy applied to normal rat brain: long-term clinical. Radiol Histopathol Anal Radiat Res 2015;184(3):314–21.
[4] Deman P, Vautrin M, Edouard M, Stupar V, Bobyk L, Farion R, et al. Monochromatic minibeams radiotherapy: from healthy tissue-sparing effect studies toward first experimental glioma bearing rats therapy. Int J Radiat Oncol Biol Phys 2012;82(4):e693–700.
[5] Prezado Y, Dos Santos M, Gonzalez W, Jouvion G, Guardiola C, Heinrich S, et al. Transfer of Minibeam Radiation Therapy into a cost-effective equipment for radiobiological studies: a proof of concept. Sci Rep 2017;7(1). https://doi.org/10.1038/s41598-017-17543-3.
[6] Bazyar S, Inscoe CR, O'Brian ET, Zhou O, Lee YZ. Minibeam radiotherapy with small animal irradiators; in vitro and in vivo feasibility studies. Phys Med Biol 2017;62(23):8924–42.
[7] Prezado Y, Sarun S, Gil S, Deman P, Bouchet A, Le Duc G. Increase of lifespan for glioma-bearing rats by using minibeam radiation therapy. J Synchrotron Radiat 2012;19(1):60–5.
[8] Gonzalez W, Dos Santos M, Guardiola C, Delorme R, Lamirault C, Juchaux M, et al. Minibeam radiation therapy at a conventional irradiator: dosimetry tools and an in vivo proof of concept. Phys Med 2020;69:256–61.
[9] Prezado Y, Jouvion G, Hardy D, Patriarca A, Nauraye C, Bergs J, et al. Proton minibeam radiation therapy spares normal rat brain: long-term clinical, radiological and histopathological analysis. Nat Sci Rep 2017;7.
[10] Adam J-F, Joubert A, Biston M-C, Charvet A-M, Peoc'h M, Le Bas J-F, et al. Prolonged survival of Fischer rats bearing F98 glioma after iodine-enhanced synchrotron stereotactic radiotherapy. Int J Radiat Oncol Biol Phys 2006;64(2):603–11.
[11] Rousseau J, Boudou C, Barth RF, Balosso J, Estève F, Elleaume H. Enhanced survival and cure of F98 glioma-bearing rats following intracerebral delivery of carboplatin in combination with photon irradiation. Clin Cancer Res 2007;13:5195–201.
[12] Vinchon-Petit S et al. External irradiation models for intracranial 9L glioma studies. J Exp Clin Cancer Res 2010;29:142–50.
[13] Montay-Gruel P, Bouchet A, Jaccard M, Patin D, Serduc R, Aim W, et al. X-rays can trigger the FLASH effect: ultra-high dose-rate synchrotron light source prevents normal brain injury after whole brain irradiation in mice. Radiother Oncol 2018;129(3):582–8.
[14] Bazalova-Carter M, Esplen N. On the capabilities of conventional x-ray tubes to deliver ultra-high (FLASH) dose rates. Med Phys 2019;46:5690–5.
[15] Perl J, Shin J, Schümann J, Faddegon B, Paganetti H. TOPAS: an innovative proton Monte Carlo platform for research and clinical applications. Med Phys 2012;39(11):6818–37.
[16] ICRP. Adult Reference Computational Phantoms. ICRP Publication 110. Ann ICRP 2009;39(2).